Enhanced transports of nutrients powered by microscale flows of self-spinning dinoflagellate *Symbiodinium*

Zheng Zhu[1] and Quan-Xing Liu[1,2,*]

1. State Key Laboratory of Estuarine and Coastal Research, School of Ecological and Environmental Sciences, East China Normal University, Shanghai 200241, China

2. Shanghai Key Lab for Urban Ecological Processes and Eco-Restoration & Center for Global Change and Ecological Forecasting, School of Ecological and Environmental Sciences, East China Normal University, Shanghai 200241, China

*To whom correspondence should be addressed. qxliu@sklec.ecnu.edu.cn

Abstract:

The metabolism of a living organism (bacteria, algae, zooplankton) requires a continuous uptake of nutrients from the surrounding environment. However, within local-spatial scales, the nutrients are quickly used up under dense concentration of organisms. Here we report that self-spinning dinoflagellate *Symbiodinium* sp. (clade E) generate a microscale flows that mitigates competition and enhances the uptake of nutrients from the surrounding environment. Our experimental and theoretical results reveal that this incessant active behavior enhances transports by about 80-fold when compared to Brownian motion in living fluids. We find that the tracers ensemble probability density function for displacement is time-dependent but consisting of a Gaussian core and robust exponential tails (so-called non-Gaussian diffusion). This can be explained by interactions of far-field Brownian motions and a near-field entrainment effect along with microscale flows. The contribution of exponential tails sharply increases with algal density, and saturates at a critical density, implying the trade-off between aggregated benefit and negative competition on the spatial self-organized cells. Our work thus shows that active motion and migration of aquatic algae play a key role

in diffusive transport and should be included in theoretical and numerical models on the physical and biogeochemical ecosystems.

Key words: **Self-spinning motion, Active fluid, Non-Brownian diffusion, Entrainment effect**

One sentence summary: Many biological studies suggest that complex and crowded environments slow down the transport from a normal diffusive behavior into a subdiffusion behavior, but our findings reveal that the diffusivity is still enhanced with a power-law behavior in actively microscale flows.

INTRODUCTION

Motile microorganisms display fascinating spatial patterns and collective behaviors evoking the focus of attention on biologist, biophysicist and ecologist in the past three decades (Bartumeus et al., 2016; Katija et al., 2012, 2015; Woodson and McManus, 2007). Especially the development of tracking techniques has motivated studies on organisms' foraging behavior from macroscale to micro- and nanoscale. Although numerous experimental observations and theoretical models have reported that the active motions of microorganisms have significant effects on their search strategies for resources such as bacteria and algal cells within aquatic environments, most of the studies are still based on a run-and-tumble-like motion behavior of organisms' themselves (Ariel et al., 2015; Bennett and Golestanian, 2013; Palyulin et al., 2014). As an extension, the entrainment effect of swimming microorganisms leading to enhanced diffusion has recently been introduced in the context of active fluids, including suspensions of swimming bacteria, mixtures of eukaryotic flagellates and ciliary beating (Guasto et al., 2011; Jeanneret et al., 2016; Leptos et al., 2009; Morozov and Marenduzzo, 2014; Shapiro et al., 2014).

Recent experimental results on swarming *Escherichia coli* bacteria revealed an enhanced diffusion of particles through the active motion of cells, namely thermal bath, as an analog to Brownian motion resulting from molecular collisions (Miño et al., 2011; Wu and Libchaber, 2000). Based on green algae *Chlamydomonas reinhardtii* systems, Leptos and collaborators demonstrated that, in dilute suspensions of the algal cells, the probability density functions of tracer displacements deviate from paradigmatic

Gaussianity, manifesting strong exponential tails (Leptos et al., 2009). Unsurprisingly, one may hypothesize that the enhanced diffusion should relate to anomalous non-Gaussian behavior, but the underpinning mechanisms remain largely elusive from experimental points of view (Bechinger et al., 2016; Hofling and Franosch, 2013). Anomalous statistical features have been found in a variety of other biological systems (Caspi et al., 2000; Freedman et al., 2017; Hofling and Franosch, 2013; Tabei et al., 2013; Wang et al., 2009). Limited experimental measurements infer that this non-Gaussian behavior is caused by the flow fields of active swimmers (Drescher et al., 2010; Guasto et al., 2010). However, the physical mechanisms underpinning non-Brownian behavior is lacking at microscale levels. A better biological model still seeks to unravel the underlying mechanisms.

Algal species have evolved ingenious ways to uptake nutrients from their aquatic environments. The common bacteria and eukaryotic flagellates use drag-enhancing flagella that help to keep run-and-tumble behaviors (Jeanneret et al., 2016; Stocker, 2011). A crucial problem for algae is how they uptake more nutrient from their local environments, in order to compete with the other algal species. Here, the complex spatiotemporal behavior of individual cells is the result of energy produced by the organisms' rotating flagella (active motility) at the microscopic scale and subsequent cascading of energy toward larger scales that greatly exceed the size of individual organisms for enhanced diffusivity and transport of nutrient particles (Barry et al., 2015; Dabiri and Gharib, 2005; Durham et al., 2013; Kokot et al., 2017; Kurtuldu et al., 2011; Woodson and McManus, 2007). Unraveling the mechanism of enhanced transports may

provide deep insights into the biological processes and sustaining mechanisms of algal blooms (Guasto et al., 2011).

Here, we investigate the statistical behavior of microscale transports on tracer particles in living fluid. Unlike previously reported biological systems such as *E. coli* and *C. reinhardtii* — swimming microorganisms that have remarkable superdiffusive behavior of translational displacement (Ariel et al., 2015; Jeanneret et al., 2016) – we studied a system with self-spinning microalgae *Symbiodinium* sp. (clade E) that do not exhibit translational displacement and found that the tracers' transport still displays a non-Gaussian Brownian motion. The overall displacement behavior is well described by a Gaussian core and exponential tails, due to the interactions of two mechanisms — the far-field Brownian motion, and the near-field entrainment effect along with fluid vortices which cause the exponential tails behavior. The enhanced diffusivity comes from the microscale vortices of spinning cells caused by cell-cell interactions, and the contribution of microscale vortices grows much faster with increased cell concentrations but saturated at the critical cell density of about 400 cells/mm^2 (volume fraction $\phi\sim$ 4.5%). We also explore this enhanced transport behavior with a simple numerical simulation, and show that the dynamic behavior is well captured by a simple microscale vorticity-diffusion process. Finally, the statistical properties of the transport displacements are studied for tracers in proximity to and far away from the nearest swimmer to give a firmer insight into the enhanced transport patterns in algal species.

MATERIALS AND METHODS

Algal cell culture and images acquisition

Free-living *Symbiodinium* sp. (clade E) are cultured in artificial seawater with F/2 medium (Guillard.1962) in a 100 ml flask, and placed in an incubator (INFORS HT Multitron pro, Switzerland). The daily cycle is 12 hours of cool light with an intensity of 2,000 Lux and 12 hours in dark at 20 °C. The algal cells in the experiments are in an exponential phase after 14 days culture and observed on the gas-liquid interface inside a disk-shaped chamber fabricated by silica gel with plastic gasket. Higher concentrations can be achieved by natural-settling about 10 times (10-20 mins each time) in a long chamber. To study the active diffusion of passive tracers influenced by the active spinning cells, milk colloid (diameter 1~2μm, Deluxe Milk, MENGNIU) is added as tracers to the suspensions (volume ratio 1:200). Visualization is performed under an inverted microscope (Nikon Ti-U) with 20× magnification objective, and a sCMOS camera (pco.edge 5.5, Germany) is used to capture the motion of cells and the tracer at 50fps for 90 sec. The observation field is about 316×316 μm^2. Image processing is performed by Matlab 2017a. The trajectories of cells and tracers are extracted from the movies through tracking programs (Zhang et al., 2010).

Flow field characterization of the PIV

The flow fields of the swimmers were qualitatively characterized by tracking the milk-collide tracers (for plastic beads will stick together in the salted sea water). We use PIVlab (Thielicke and Stamhuis, 2014) (version 1.5) to analyze a series of continuous pictures taken at 50 frames per second. Before loading into the PIVlab, we use top-hat transform and mask all of the swimmers as the pre-process of the pictures. After getting a series of instant velocity field, we take the average of a rotational period to get a mean flow fields generated by the spinning of the cells and normalize vorticity by the maximum to denote the orientation of the flow. Positive value means counter-clockwise flow while negative value means clockwise flow. To characterize the difference between flow states, we use spatial velocity-velocity correlation functions. $C_{vv}(r) = \langle v_i \cdot v_j \rangle_{|\overline{r_j}-\overline{r_i}|=r, j\geq i}$, where $\overline{r_i}$ are the positions of the velocity, i and j are the indices running over all vectors. The normalized $C_{vv}(r)$ curves show strong negative correlation in the microvortex while decline to zero fast in turbulent flows.

The near-field and far-field calculations

In order to separate the contribution of active part from the passive Brownian motion, we set a threshold at ~35 μm, relating to the spinning center. The length is a bit larger than the sum of the rotating radius and one body size, which confirms to the scale of a micro-vortexes, then we recalculate the PDFs of displacement according to the nearest distance of particles and the spinning center. So that the pdf is decomposed into two parts, the near-field part (distance < 35 μm) and the far-field (distance > 35 μm) part.

RESULTS

Density-dependent turbulence and active transport

Symbiodinium sp. (clade E) are unicellular with body size $d \approx 12 \pm 3\ \mu\mathrm{m}$ in diameter and possess two dissimilar flagella arising from the ventral side (one longitudinal flagellum and one transverse flagellum) that are responsible for a rotational speed $\omega \approx 15 \pm 5\ \mathrm{rad/s}$, according to our lab experimental measurements. The transport of nutrients in living fluids without external pressure is composed of intrinsic diffusion and active transport processes induced by microorganisms. The trajectories of particles influenced by microorganisms can be divided into three composition: intrinsic Brownian motions, circle-like behavior induced by hydrodynamics and entrainment effects caused by a collision with active swimmers. The self-spinning *Symbiodinium* cell can create large vortex patterns if their concentration is sufficiently high (Fig. 1A, B). With increasing algal density, the near-field effect of the vortical flow gradually governs the entire hydrodynamics (Fig. 1). Then large vortexes merge together to forming microscale turbulences, where intrinsic Brownian motion effects become less important to nutrient transport comparing with the collision-dominated high-density regime (Fig. 1C, D). These microscale turbulences lead to a long-range transport that have profound effects on nutrient mixing and molecular transport in microbiological systems.

Video microscopy reveals that density of self-spinning cells control the spatial scale of the vortical flow (inset of Fig. 1A and supplemental movie S1) and the displacement of tracers (Fig. 1C, D) in *Symbiodinium* systems. The coarse-grained

mean velocity field averaged by an algal rotating period (about 0.24 sec) are shown in Fig. 1A, B under a low and high density respectively (see supplemental movie S1). At low density, the spatial correlation (27), $C_{vv}(r)$ of the velocity vectors as a function of the distance r, has a minimum at $r \approx 34\,\mu m$ corresponding to the approximate diameter of a vorticity generated by a spinning cell (inset of Fig. 1A), contrasting with a rapid decline and small vortical scale at high density.

Based on the velocity analysis of the fluid field, we hypothesized that a single spinning *Symbiodinium* cells can only attract tracers (nutrient particles) around itself (within radius R) through a vortical flow, whereas the transport dynamics are enhanced through the collective self-spinning behavior. Experimental results directly support this hypothesis shown in Fig. 2 (see supplemental movie S2). At high density, the tracers are no longer fixed around one algal cell, but drifted among the algal cells instead. Moreover, in our experiments, a few particles will be pulled towards the algae when the distance is closer than a critical radius R (~30μm) towards the self-spinning center. It is intuitive that the particle moves much further in the 'algal bath' rather than fixed around by a single cell. This active transport implicates an enhanced diffusion mechanism and uncovers the potential benefits of collective spinning behavior despite the existence of strong intra-species competition between algal cells.

Departures from gaussianity and underlying mechanisms

In order to quantify the displacement behavior of the enhanced transport in living fluids, firstly, we measure the displacement of Δx in the 'algal bath' and calculate the probability density function of the tracers' displacements $P(\Delta x, \Delta t)$ along an arbitrary

direction for a number of increasing time intervals Δt. Probability density functions (PDFs) of the in-plane tracers displacements coincide with formula (Leptos et al., 2009),

$$P(\Delta x, \Delta t) = \frac{1-f}{(2\pi\delta_g^2)^{1/2}} e^{-(\Delta x)^2/2\pi\delta_g^2} + \frac{f}{2\delta_e} e^{-|\Delta x|/\delta_e}. \quad (1)$$

Equation (1) can be seen as a weighted sum of Gaussian and exponential distributions. f describes the contribution of the exponential tails, and δ_e represents the characteristic decay length of transport displacements due to the entrainment effect.

Without swimmers (*Symbiodinium* cells), tracers (nutrient particles) undergo pure Brownian motions, and exhibit accurate Gaussian behavior, whereas with the presence of active spinning cells in the fluid, the exponential tails appear (Fig. 3A). At a fixed interval $\Delta t = 0.24$ sec (the algal rotating period), the PDFs reveal a broadening of the Gaussian core and a growth of the magnitudes of exponential tails with increasing cell density. As shown in Fig. 3B, the PDFs collapse to form a master curve implying the general scale-law behavior independent on the time. This qualitative behavior coincides with the previous studies in thin films of swimming bacteria and microalgae displaying a run-and-tumble behavior (Jeanneret et al., 2016; Leptos et al., 2009). However, in contrast to run-and tumble behavior, we elucidate this exponential tail behavior results from the near-field entrainments effect in our spinning biological systems (Fig. 3C and Fig. S2). With varying densities, the near-field displacement PDFs collapse to a master scaling again, and display the same magnitudes of the exponential tails and the width of Gaussian core; the far-field displacement shows a same width of Gaussian distribution. The results in turn are robust for the various intervals at $\Delta t = 1.2$ sec and $\Delta t = 2.4$ sec (see Fig. S1) although the near-field displacement seems to not

approach a Gaussian distribution with increasing time intervals, but it still shows the broadening of Gaussian core, which indicates that the enhancement of the transport is dominated by the near-field entrainment along with fluid flows driven by the active spinning *Symbiodinium* cells.

Enhanced transport and diffusive scaling

The broadening of the PDFs with cell density indicate significantly enhanced transport. To quantify this behavior, we use the mean square displacement (MSD) of particles for varying cell densities to describe the scaling law of spatial dispersal, with the expression $\mathrm{MSD}(\Delta t) = \langle |r(t+\Delta t) - r(t)|^2 \rangle$, where the brackets denote an ensemble average over thousands of particles. We observed that $\mathrm{MSD} \sim \Delta t^{\alpha}$ with α=1.0 for absence of spinning cells at all time, which agrees with expected a normal diffusion behavior. Whereas if the density increases, the diffusive regime shows an anomalous transport behavior in which the exponent α gradually increases from 1.0 to 1.5 (Fig. 4A).

To elucidate the origin of observed anomalous diffusion, we further quantify the contribution of the near-field entrainment and far-field motion to MSD and PDFs through the parameters of equation (1). As one sees from Fig. 4B, the anomalous diffusion behavior comes from the near-field entrainment effect that driven by a microscale vortical flow. With the increasing density, the fraction of exponential tail reveals a nonlinear density-dependent relationship (Fig. 4C), and it is saturation at the value of about 0.5 for cell densities above about 400 cells/mm^2 (volume fraction $\phi \sim$ 4.5%). Going beyond this critical density, the nearest distance between the algal cells are close to 35μm, then the interaction is fully dominated by the entrainment effects

along with the near-field hydrodynamics. The continued growth of the spatial decay length imply that the tracers frequently jump from one vortical flow to other vortexes with an increasing density (Fig. S2). It is obvious that the strength of the entrainment effects also grows with the increasing active cells density.

For a micro-particle exhibiting Brownian motion in two dimensions, the MSD is proportional to Δt, following MSD$\sim 4D_e\Delta t$ for $\Delta t \gg \tau$, where τ is a characteristic correlation time. For pure Brownian motion alone, the diffusion coefficients should be $D_0 = k_B T/6\pi\eta a$ resulting from Stokes-Einstein relation of spherical particles through a liquid with low Reynolds number (Einstein, 1905). Here k_B, T, η and a are Boltzmann's constant, the absolute temperature, the dynamic viscosity, and the particle radius respectively. Substituting the following values into the equation of D_0, $T = 297.65K$, $\eta = 1.2 \times 10^{-3} Pa \cdot s$, $a \approx 0.75\,\mu m$ (mean), we can obtain $D_0 = 0.218\,\mu\mathrm{m}^2/\mathrm{s}$, which is a good agreement with experimental value $0.229\,\mu\mathrm{m}^2/$ s underlying absence of active spinning cells. The effective diffusion coefficients follow a power law with exponent 1.23 as active algal density increases (Fig.4D). This is different comparison with previous reported in active bacterial living fluids displaying a linear relation (Leptos et al, 2009).

To gain additional insights on entrainment-induced transport in active spinning cells, we explore the movement speed of the tracers along the Stokes flow around a cell. Fig. 5A depicts an experimental trajectory tracking of a tracer, showing the tracer oscillations, powered by the microscale vortexes, which are enhanced as the tracer gets closer to the rotating cell in a frame of reference moving with the algal cell. These

enhanced amplitudes of velocities suggest a long persistent length and time within a vortex (Fig. 5B) at a high cell density, i.e. trapped by the vortex. Note that the observed trajectories are twisted if the particle is beyond the critical distance, whereas it shows a zig-zag feature of the trajectories at the critical distance (Fig. 2 and supplemental movie S2). The radial velocity of the tracer further confirms that it is dominated by Brownian motion to near-field entrainment transport along with near-field hydrodynamics; and the velocity distributions display typical unimodal and bimodal patterns at far-field and near-field hydrodynamics respectively.

Theoretical model

We model the passive particles as spheres immersed in the concentration field with active spinning cells. The two-dimensional projection of the stochastic trajectory of a particle in the lab experiments, $(X(t), Y(t))$, can be expressed as

$$\begin{cases} dX(t) = \sqrt{2D_W}\, dW_X(t) + (L\cos\theta + A\cos\varphi)dt \\ dY(t) = \sqrt{2D_W}\, dW_Y(t) + (L\sin\theta + A\sin\varphi)dt \cdot \\ d\theta(t) = \omega dt + K dP(t) \end{cases} \quad (2)$$

The stochastic equations integrate the standard Wiener processes $dW_{X,Y}(t)$ of Brownian motion with diffusivity D_W (without active particles), and a small displacement with $\varphi(t+T) = -\varphi(t)$, caused by the near-field entrainment effect of the fluid vortices, and finally with a Poisson process for the jumps from one vortical flow of a swimmer to another one $dP(t)$. T denotes a half of tracer's turning period (~0.12 sec). L and A denote the arc length (per step) caused by the tangential force and radial force generated by the spinning motion respectively. These dynamics are

simulated using a time step $\Delta t = 0.02$ sec, the same as the experimental measurements.

Our theoretical simulations suggest that the random walks with diffusivity D_W has little impact on the final trajectories, because the effective turbulent transport is up to 80-fold larger than the Brownian motion of microparticles in diffusivity. The produced trajectories of model (2) coincide well with the experimental ones at high densities (Fig. S3). The simulation predicts the zig-zag behavior and circular motion around one algal cell switch to another for the partials, and is in remarkable agreement with our experimental estimates of $P(\Delta x, \Delta t)$ and MSD, as shown in Fig. 3A and Fig. 4A.

DISCUSSION

Microorganisms play an important role in trophic dynamics and biogeochemistry of marine ecosystems through collective and motile behaviors, as their concentrations and activities often peak at localized hotspots (Doostmohammadi et al., 2012). Generally, the negatively-buoyant and non-motile cells like diatoms are dependent on turbulence to keep resuspending them into the photic zone, while the motility of dinoflagellates allow the cell to control its vertical position on resource requirements such as light that more abundant at the surfaceand nutrient rich areas (Ross and Sharples, 2007). Dinoflagellates *Symbiodinium* cells are thought to have lower photosynthetic rates, higher metabolic costs and nutrient affinity coefficients than diatoms (Smayda, 1997), so *Symbiodinium* cells evolve a unique motility to symbiosis with coral reefs. Numerous algae species possess different motile patterns and survival strategies to coping with

nutrient-depleted conditions (Jeong et al., 2012). However, besides foraging nutrients directly, hydrodynamic cell–cell interactions that grow more relevant as the cell density increases have been so far ignored in numerous literature (Breier et al., 2018).

Here, we have shown that the statistics of passive-tracer displacements in suspensions of spinning microalgae *Symbiodinium* sp. (clade E) exhibit a Gaussian core with exponential tails due to the near-field entrainment effect driven by the vortical flows. This argument is supported both experimental and theoretical results with extracted tracers close to the active spinning cells. Through calculation of the effective diffusion coefficients, we find that an effective turbulent transport is up to 80-fold larger than the Brownian motion of microparticles in seawater and the contribution of microscale vortices grows much faster with increased algal density but saturated at the critical density of about 400 cells/mm^2 (volume fraction φ~4.5%). The integrated model with the far-field Brown-motion and the near-field entrainment effect further implicates the enhanced transport behavior of particles at a high algal density.

In our experiments, the *Symbiodinium* sp. density is range from 0% to 10%, much higher than the experiments on green algae *Chlamydomonas reinhardtii* (Leptos et al., 2009 and Jeanneret et al., 2016) with a maximum about 2.2%, which can account for the appearance of the saturation. At the critical density, the mean distance of its nearest neighbor is close to 40 μm which almost equals to the microvortex scale 34 μm – a *Symbiodinium* sp. cell can generate. Below the critical density, the random walk of the nutrient would prevail for the distance is too large for *Symbiodinium* cells to interact with each other. Moreover, the maximum density in culture without concentrating can

only arrive up to 5 ~ 6% – a bit larger than the critical value. This may suggest a tradeoff between collective behaviors of enhanced transport and individual uptake within the flows.

Comparing with existed studies on microalgae (Jeanneret et al., 2016), bacterial (Jeanneret et al., 2016), and synthetic microswimmers (Kokot et al., 2017) performing "run-and-tumble" behaviors in the suspensions, the entrainment effects and enhanced transport mainly arise from the collisions between the microparticles and the swimmers. However, our experimental results showed that the enhanced transport could origin from stable vortical flows generated by spinning behavior. This stable vortex would make a nematic arrangement to embedding largest number of algal cells, but minimize the cost of energy consumption. Moreover, because of the spinning feature of the algal cells, the entrainment effect generates a long-range transport more easily at a high density rather than a low density.

Acknowledgments

We thank Fang Shen for her generosity in sharing the algae *Symbiodinium* sp. (clade E). strain, Wen-Si Hu assistant the experiments and He-Peng Zhang for very helpful discussions on the experimental setup. This research was financially supported by the National Key R&D Program of China (2016YFE0103200), the National Natural Science Foundation of China (41676084).

References

Ariel, G., Rabani, A., Benisty, S., Partridge, J. D., Harshey, R. M. and Be'er, A. (2015). Swarming bacteria migrate by Lévy walk. *Nature Communications* **6**, 8396.

Barry, M. T., Rusconi, R., Guasto, J. S. and Stocker, R. (2015). Shear-induced orientational dynamics and spatial heterogeneity in suspensions of motile phytoplankton. *J. R. Soc. Interface* **12**, 20150791.

Bartumeus, F., Campos, D., Ryu, W. S., Lloret-Cabot, R., Méndez, V. and Catalan, J. (2016). Foraging success under uncertainty: Search tradeoffs and optimal space use. *Ecology Letters* **19**, 1299-1313.

Bechinger, C., Di Leonardo, R., Löwen, H., Reichhardt, C., Volpe, G. and Volpe, G. (2016). Active particles in complex and crowded environments. *Reviews of Modern Physics* **88**, 045006.

Bennett, R. R. and Golestanian, R. (2013). Emergent run-and-tumble behavior in a simple model of *Chlamydomonas* with intrinsic noise. *Phys. Rev. Lett.* **110**, 148102.

Breier, R. E., Lalescu, C. C., Waas, D., Wilczek, M. and Mazza, M. G. (2018). Emergence of phytoplankton patchiness at small scales in mild turbulence. *Proc. Natl. Acad. Sci. USA* **115,** 12112-12117

Caspi, A., Granek, R. and Elbaum, M. (2000). Enhanced diffusion in active intracellular transport. *Phys. Rev. Lett.* **85**, 5655-5658.

Dabiri, J. O. and Gharib, M. (2005). The role of optimal vortex formation in biological fluid transport. *Proc. R. Soc. B* **272**, 1557.

Doostmohammadi, A., Stocker, R. and Ardekani, A. M. (2012). Low-Reynolds-number swimming at pycnoclines. *Proc. Natl. Acad. Sci. USA* **109,** 3856-3861.

Drescher, K., Goldstein, R. E., Michel, N., Polin, M. and Tuval, I. (2010). Direct measurement of the flow field around swimming microorganisms. *Phys. Rev. Lett.* **105**, 168101.

Durham, W. M., Climent, E., Barry, M., De Lillo, F., Boffetta, G., Cencini, M. and Stocker, R. (2013). Turbulence drives microscale patches of motile phytoplankton. *Nature Communications* **4,** 2148.

Einstein, A. (1905). Investigations on the theory of Brownian movement. *Annalen der Physik* **17**, 549-560.

Freedman, S. L., Banerjee, S., Hocky, G. M. and Dinner, A. R. (2017). A versatile framework for simulating the dynamic mechanical structure of cytoskeletal networks. *Biophysical Journal* **113**, 448-460.

Guasto, J. S., Johnson, K. A. and Gollub, J. P. (2010). Oscillatory flows induced by microorganisms swimming in two dimensions. *Phys. Rev. Lett.* **105**, 168102.

Guasto, J. S., Rusconi, R. and Stocker, R. (2011). Fluid mechanics of planktonic microorganisms. *Annu. Rev. .Fluid Mech.* **44**, 373-400.

Hofling, F. and Franosch, T. (2013). Anomalous transport in the crowded world of biological cells. *Rep. Prog. Phys.* **76**, 046602.

Jeanneret, R., Pushkin, D. O., Kantsler, V. and Polin, M. (2016). Entrainment dominates the interaction of microalgae with micron-sized objects. *Nature Communications* **7**, 12518.

Jeong, H. J., Yoo, Y. D., Kang, N. S., Lim, A. S., Seong, K. A., Lee, S. Y., Lee, M. J., Lee, K. H., Kim, H. S., Shin, W. et al. (2012). Heterotrophic feeding as a newly identified survival strategy of the dinoflagellate *Symbiodinium*. *Proc. Natl. Acad. Sci. USA* **109**, 12604-12609.

Katija, K., **Colin, S. P., Costello, J. H. and Jiang, H.** (2015). Ontogenetic propulsive transitions by *Sarsia tubulosa* medusae. *J. Exp. Biol.* **218**, 2333-2343.

Katija, K. (2012). Biogenic inputs to ocean mixing. *J. Exp. Biol.* **215**, 1040.

Kokot, G., Das, S., Winkler, R. G., Gompper, G., Aranson, I. S. and Snezhko, A. (2017). Active turbulence in a gas of self-assembled spinners. *Proc. Natl. Acad. Sci. USA* **114**, 12870.

Kurtuldu, H., Guasto, J. S., Johnson, K. A. and Gollub, J. P. (2011). Enhancement of biomixing by swimming algal cells in two-dimensional films. *Proc. Natl. Acad. Sci. USA* **108**, 10391.

Leptos, K. C., Guasto, J. S., Gollub, J. P., Pesci, A. I. and Goldstein, R. E. (2009). Dynamics of enhanced tracer diffusion in suspensions of swimming eukaryotic microorganisms. *Phys. Rev. Lett.* **103**, 198103.

Lauga, E. and Powers, T.R. (2009) The hydrodynamics of swimming microorganisms, *Rep. Prog. Phys.* **72**, 096601.

Miño, G., Mallouk, T. E., Darnige, T., Hoyos, M., Dauchet, J., Dunstan, J., Soto, R., Wang, Y., Rousselet, A. and Clement, E. (2011). Enhanced diffusion due to active swimmers at a solid surface. *Phys. Rev. Lett.* **106**, 048102.

Morozov, A. and Marenduzzo, D. (2014). Enhanced diffusion of tracer particles in dilute bacterial suspensions. *Soft Matter* **10**, 2748-2758.

Palyulin, V. V., Chechkin, A. V. and Metzler, R. (2014). Lévy flights do not always optimize random blind search for sparse targets. *Proc. Natl. Acad. Sci. USA* **111**, 2931-2936.

Ross, O. N. and Sharples, J. (2007). Phytoplankton motility and the competition for nutrients in the thermocline. *Marine Ecology Progress Series* **347**, 21-38.

Shapiro, O. H., Fernandez, V. I., Garren, M., Guasto, J. S., Debaillon-Vesque, F. P., Kramarsky-Winter, E., Vardi, A. and Stocker, R. (2014). Vortical ciliary flows actively enhance mass transport in reef corals. *Proc. Natl. Acad. Sci. USA* **111**, 13391.

Stocker, R. (2011). Reverse and flick: Hybrid locomotion in bacteria. *Proc. Natl. Acad. Sci. USA* **108**, 2635-2636.

Smayda, T. J. (1997). Harmful algal blooms: Their ecophysiology and general relevance to phytoplankton blooms in the sea. *Limnol. and Oceanogr.* **42**, 1137-1153.

Tabei, S. M. A., Burov, S., Kim, H. Y., Kuznetsov, A., Huynh, T., Jureller, J., Philipson, L. H., Dinner, A. R. and Scherer, N. F. (2013). Intracellular transport of insulin granules is a subordinated random walk. *Proc. Natl. Acad. Sci. USA* **110**, 4911-4916.

Thielicke, W. and Stamhuis, E. J. (2014). PIVlab–Towards user-friendly, affordable and accurate digital particle image velocimetry in MATLAB. *Journal of Open Research Software* **2**, p.e30.

Wang, B., Anthony, S. M., Bae, S. C. and Granick, S. (2009). Anomalous yet Brownian. *Proc. Natl. Acad. Sci. USA* **106**, 15160-15164.

Woodson, C. B. and McManus, M. A. (2007). Foraging behavior can influence dispersal of marine organisms. *Limnol. and Oceanogr.* **52**, 2701-2709.

Wu, X. L. and Libchaber, A. (2000). Particle diffusion in a quasi-two-dimensional bacterial bath. *Phys. Rev. Lett.* **84**, 3017-3020.

Zhang, H. P., Be'er, A., Florin, E. L. and Swinney, H. L. (2010). Collective motion and density fluctuations in bacterial colonies. *Proc. Natl. Acad. Sci. USA* **107**, 13626-13630.

Figures

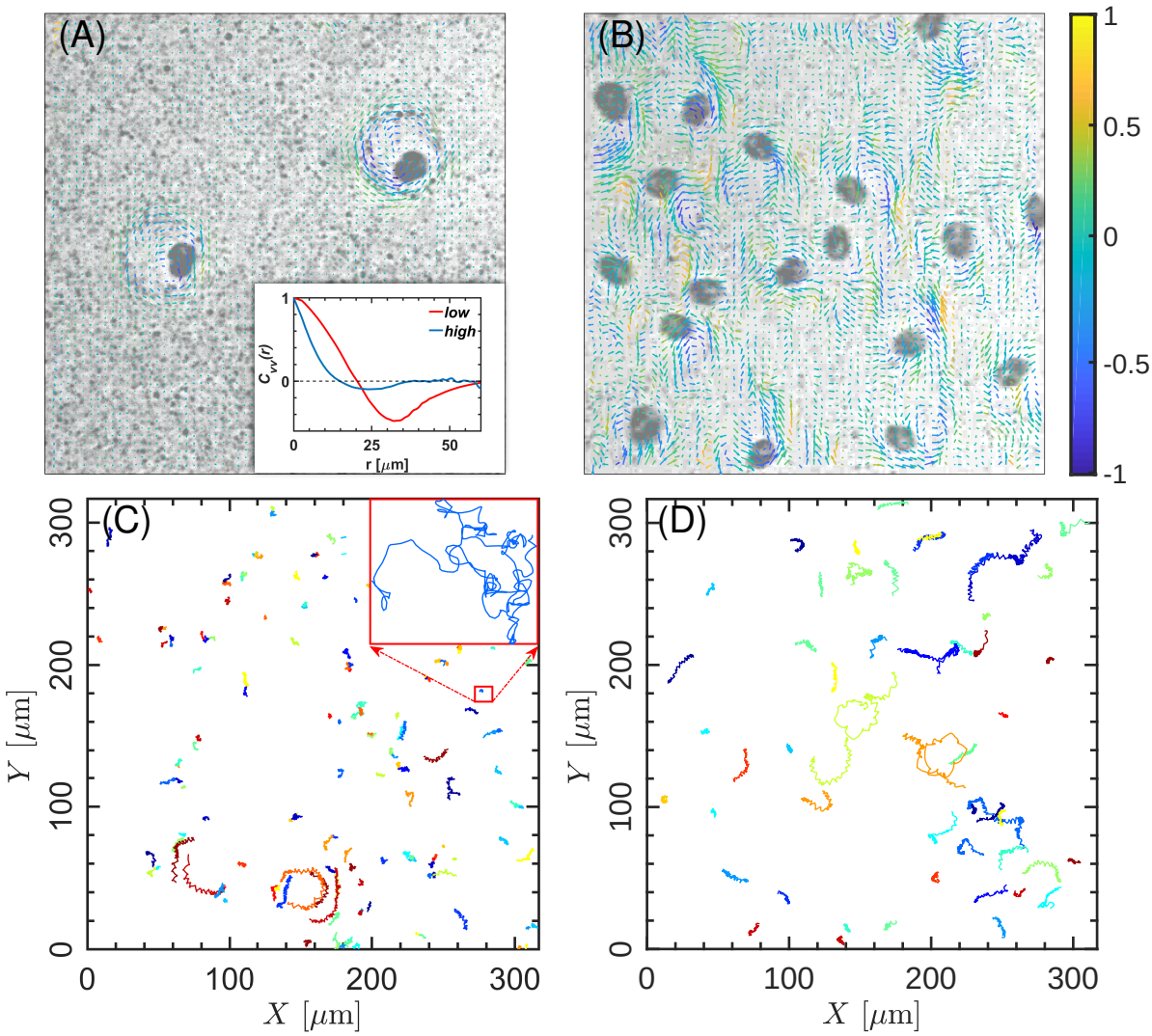

Figure 1. Experimental observations of the spatial microscale turbulence. (A) Snapshots of the coarse-grained velocity field generated in one rotation period (≈0.24 sec), calculated by matlabPIV (see Materials and Methods for details, coarse graining length Δl=2.64 μm), obtained from situ measurement with tracers at low algal density (see supplementary video S1). (B) Microscale turbulent state dominates the transport patterns on tracers at high algal densities with the same method of (A). Colored arrows show fluid flow direction distinguished by normalized local vorticity, $\vec{\omega} = \nabla \times \vec{v} = \partial_x v_y - \partial_y v_x$. The spatial scale is about 165 microns. (C, D) Spatial dispersals of tracers at low- and high -cell density respectively, where Brownian motion of particles dominates the transport patterns (C), compared with the entrainment effect along with fluid turbulence becoming dominant, which caused by the active swimmers (D). All the trajectories were randomly picked by a 40sec interval and only a few tracers were shown for clarity.

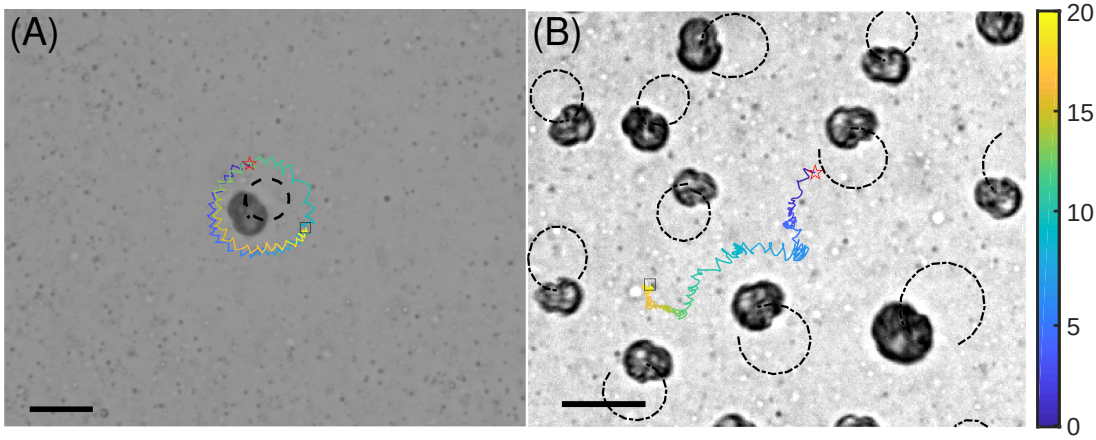

Figure 2. Density-dependent transport behavior of nutrient particles in microscale flows generated by self-spinning algal cells. The illustrations show the different behaviors of nutrient particles driven by the near-field hydrodynamics in active living fluids: entrainment motion (A) at low algal density and enhanced transport (B) at high algal density. The dashed circular orbits represent the trajectories of active algal cells with radius R, and the colored solid lines describe the trajectories (plotted over 20 sec) of nutrient particles along with turbulent flows. The red stars and square symbols represent the position of the initial time and the end time, coming from experimental measurement (see supplementary video S2). Scale bars, 20 microns.

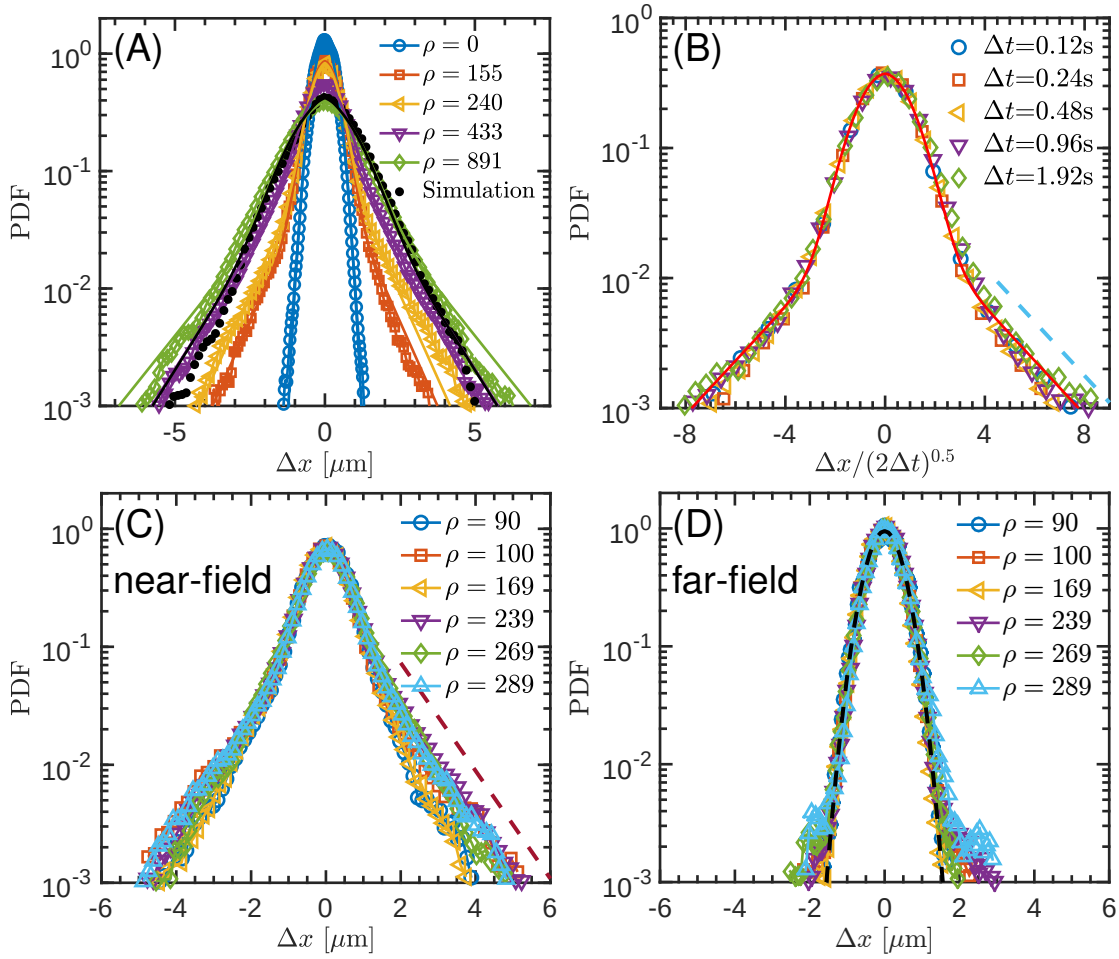

Figure 3. Probability density functions (PDFs) for tracer displacements. (A) Ensemble PDFs, for various densities of active algal cells, showing the broadening of the Gaussian core and emergence of exponential tails. Eq. (1) was used to obtain the relative contribution of the enhanced displacements results from the near-field entrainment effect and vortical flows comparison with far-field Brownian motion. Black dots are results of the simulation at high density. (B) Diffusive rescaling of PDFs at $\rho = 90$ cells/mm^2 and various time intervals shows an exponential-tail behavior with a slope -0.48, illustrating data collapse to the master scaling law. (C, D) Overlaid PDFs of displacements of tracer particles associated with various algal densities at a near-field exponential-tail behavior with a slope -1.05 (C) and at a far-field Gaussian core behavior (D) respectively. All statistical displacements were at a fixed time interval $\Delta t = 0.24$ sec (a rotational period) but varying time for (B).

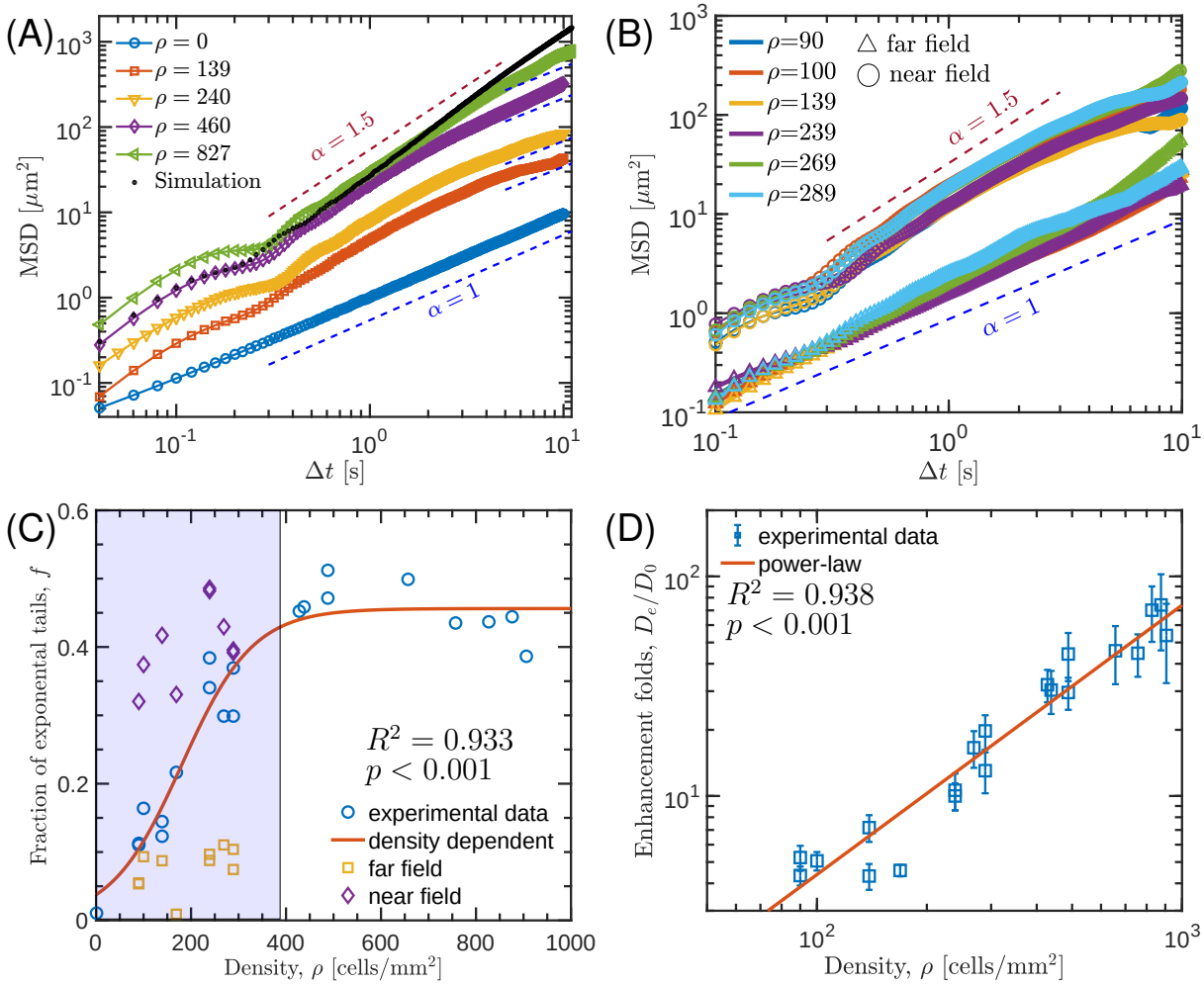

Figure 4. Enhanced diffusional properties of tracer particles affected by active algal density. (A) MSDs of the tracers versus time at various active algal densities (microscale vortexes), showing diffusive scaling behavior with the increasing of time scales. The motion behaviors shift from Brownian diffusion to super-diffusion by increasing density of the algal cell at long-term scales. Black dots are result of the simulation at high density. (B) MSDs of various algae densities separating into near-field (circles) and far-field (triangles), the statistical distances also take the threshold at 35 μm relative to the spinning center. (C, D) Density-dependent enhanced effect of the exponential tails contribution (C) and enhancement factor (D) calculated from the behaviors of PDFs in two-dimensional experimental data, where the solid curves imply the nonlinear saturation function and the scaling law of $\Phi = \frac{D_e}{D_0} \approx \rho^{1.23}$ to fit the experimental data. Error bars represent standard deviations. The regressions curves are statistically significant ($p < 0.001$) and have R^2 values corresponding to 0.933 and 0.938, respectively.

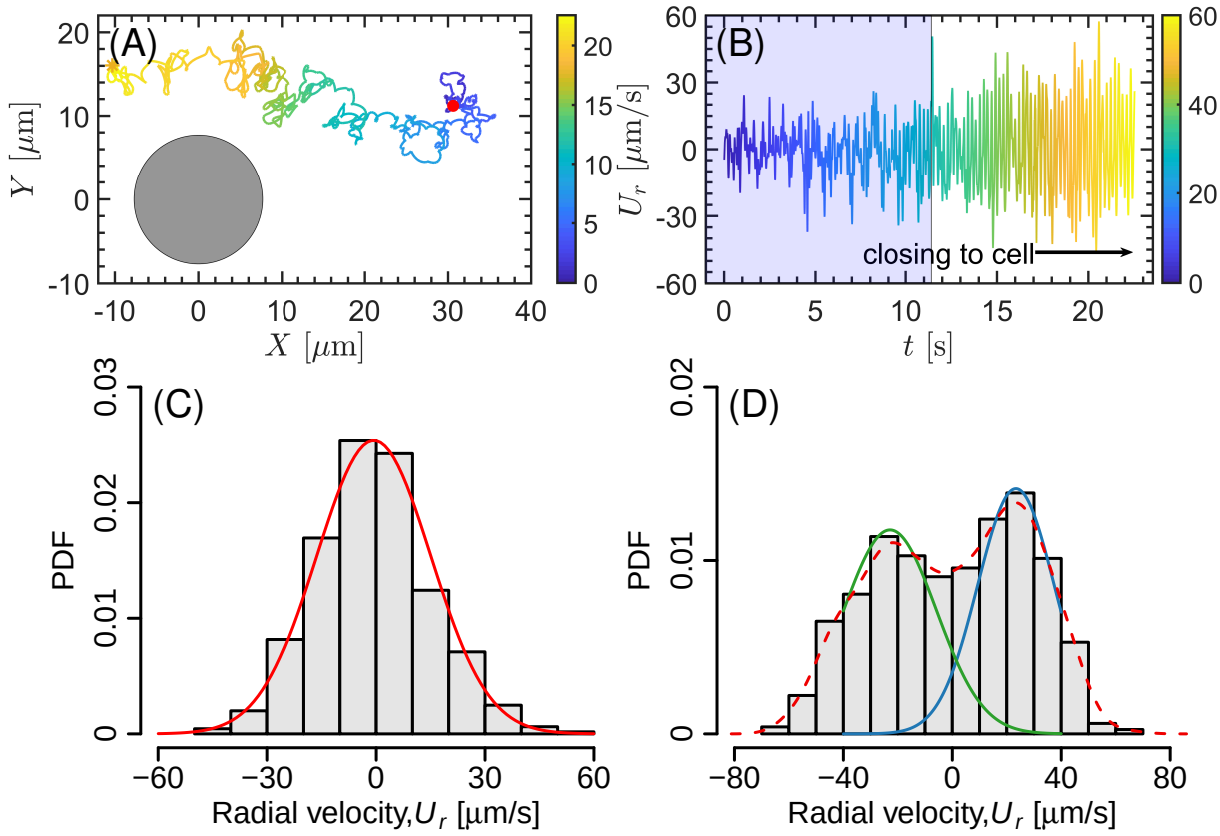

Figure 5. Dynamics behaviors of tracers within active fluids. (A) Trajectory of a tracer underlies enhanced diffusion scenarios powered by microscale vortexes arising from rotational algal cells. (B) The radial velocity of the tracer was dominated by Brownian motion to near-field entrainment transport along with near-field hydrodynamic generated from the rotating cell, where the radial velocity remarkably shifts to the periodic-like oscillation and enlarged amplitude close to the cells. Black disks represent the approximate size of the rotated circle of an algal cell. (C, D) The typical unimodal and bimodal distributions at a far-field Brownian motion and near-field enhanced diffusion respectively, where the solid curves are Gaussian fits to the data of radial velocity U_r.

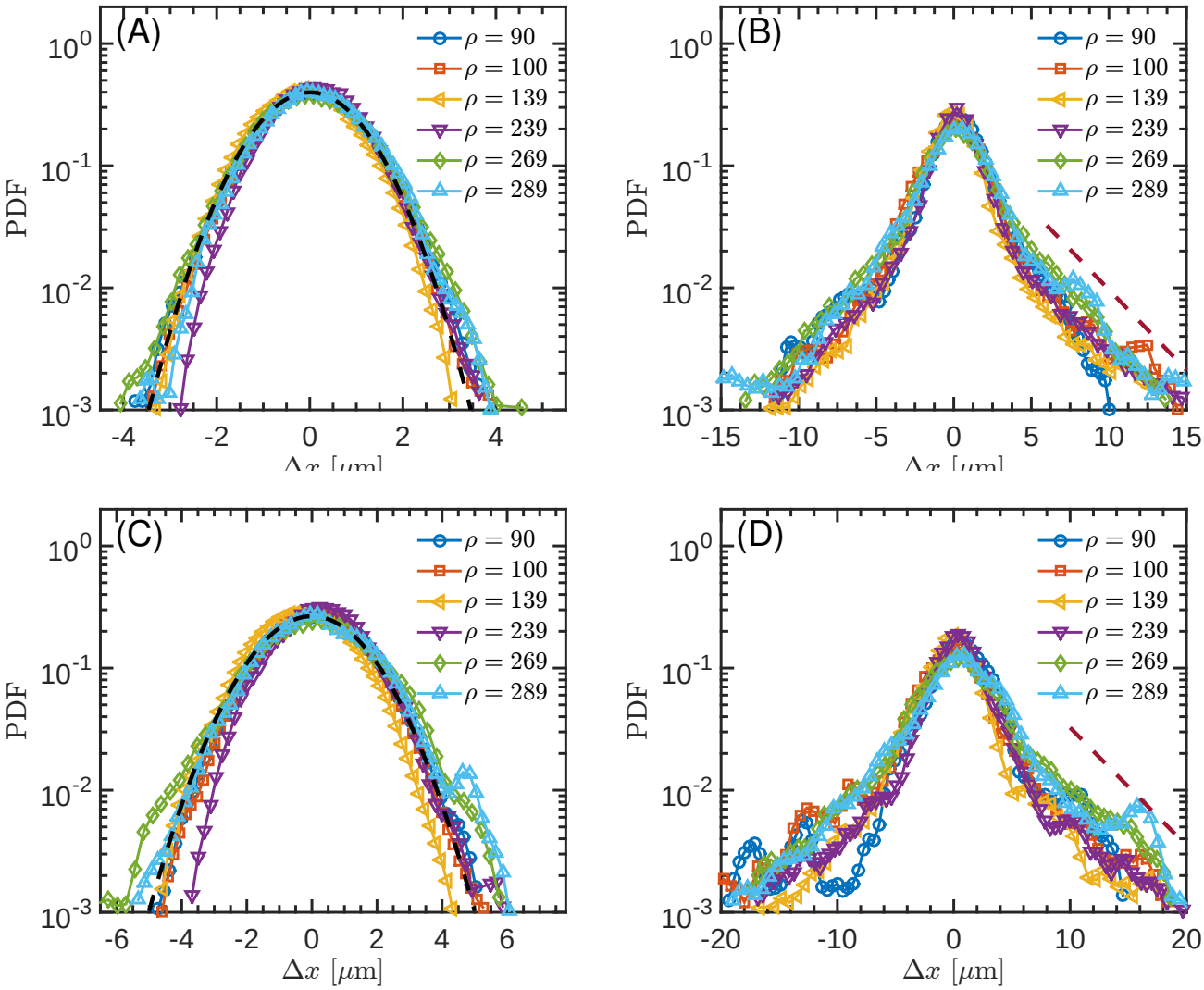

Fig. S1. Probability density functions (PDFs) for tracer displacements. Overlaid PDFs of displacements of tracer particles associated with various algal densities on far-field Gaussian core behavior (A, C) and near-field exponential-tails behavior (B, D) with a slope $k = -0.30$ and $k = -0.22$ respectively. The statistical distances take the threshold at 35 μm (about 2-fold body sizes) relative to the center of spinner circles. (A, B) Time interval $\Delta t = 1.2$ sec and (C, D) $\Delta t = 2.4$ sec.

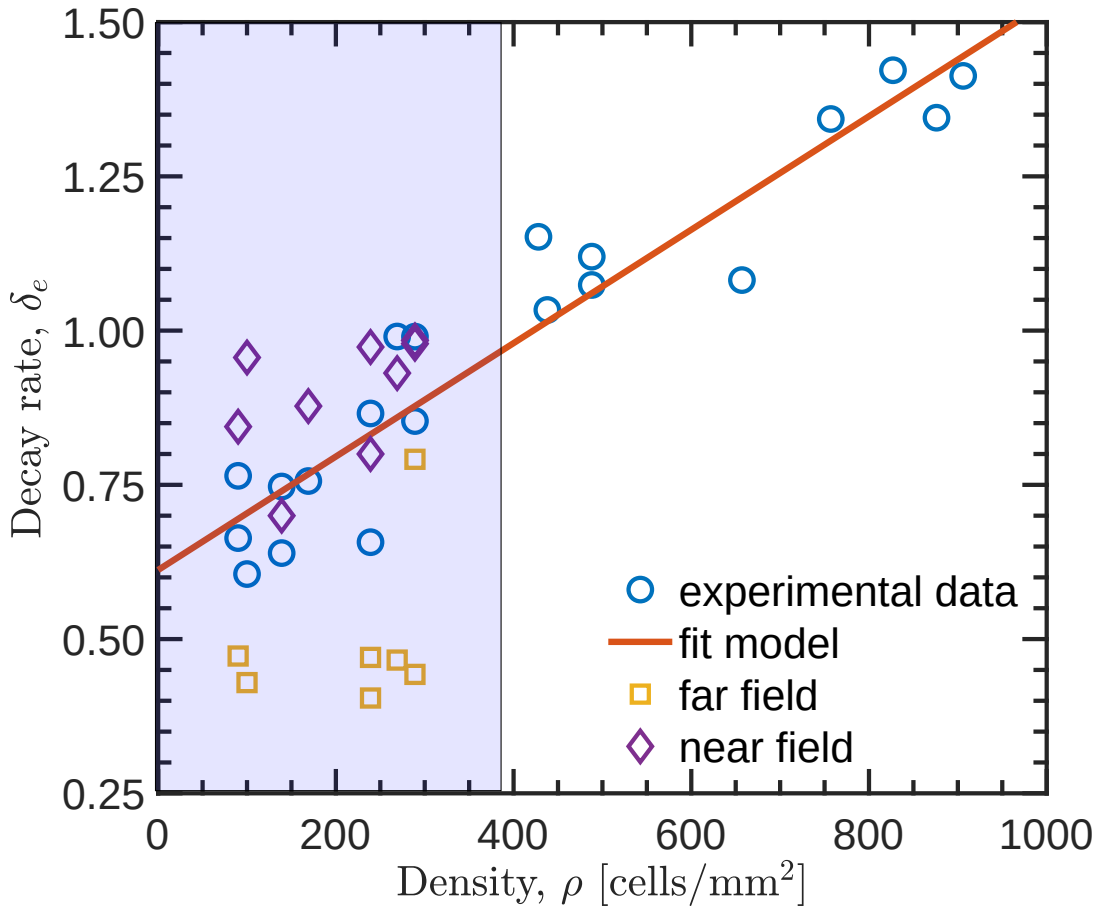

Fig. S2. Spatial decay rates of turbulence caused by the 'algal bath'. The relationship of decay rate of long exponential-tail PDFs with increasing packing density of active algal cells. The solid line represents a best linear fit to the data with a slope 7.689. The regressions curve is statistically significant ($p < 0.001$) and has R^2 value corresponding to 0.900.

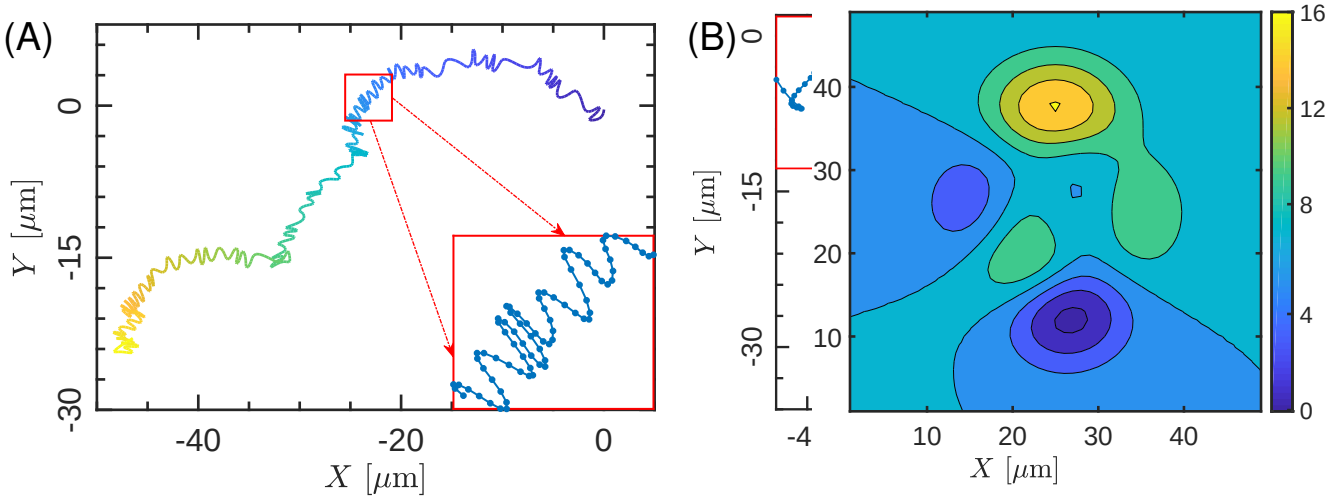

Fig. S3. Trajectories at high algal density. (A) The results of simulation solved by the stochastic differential equation (2) comparison with the real experiment trajectories (B). The model well captures the transport behavior, and suggest that the enhanced transport understand with the interage of Brownian motion and Poisson events entrainments.

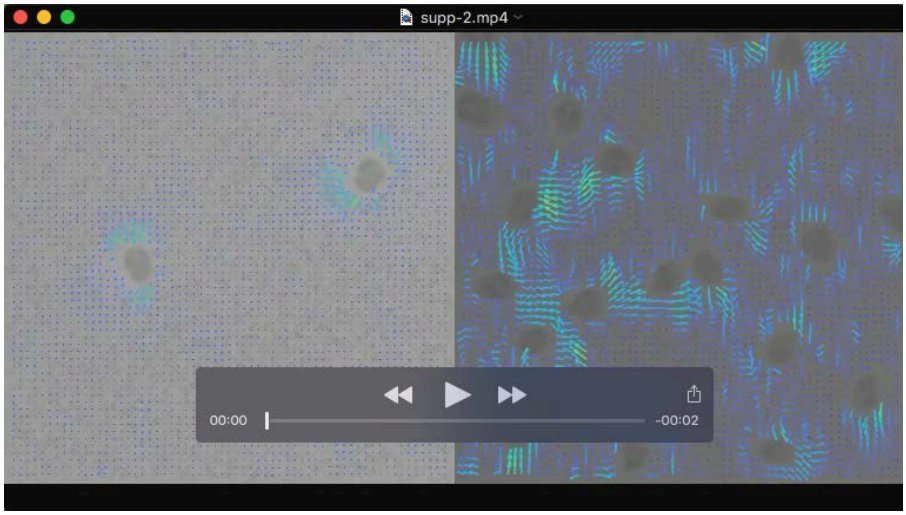

Movie 1. Instant velocity field analyzed by PIVLAB package. The size of the visual fields is 165 μm by 165 μm and the coarse graining length Δl=2.64μm. The video is played 3.5 times slower. (left) and (right) corresponding to Fig. 1(A) and (B) in the main context.

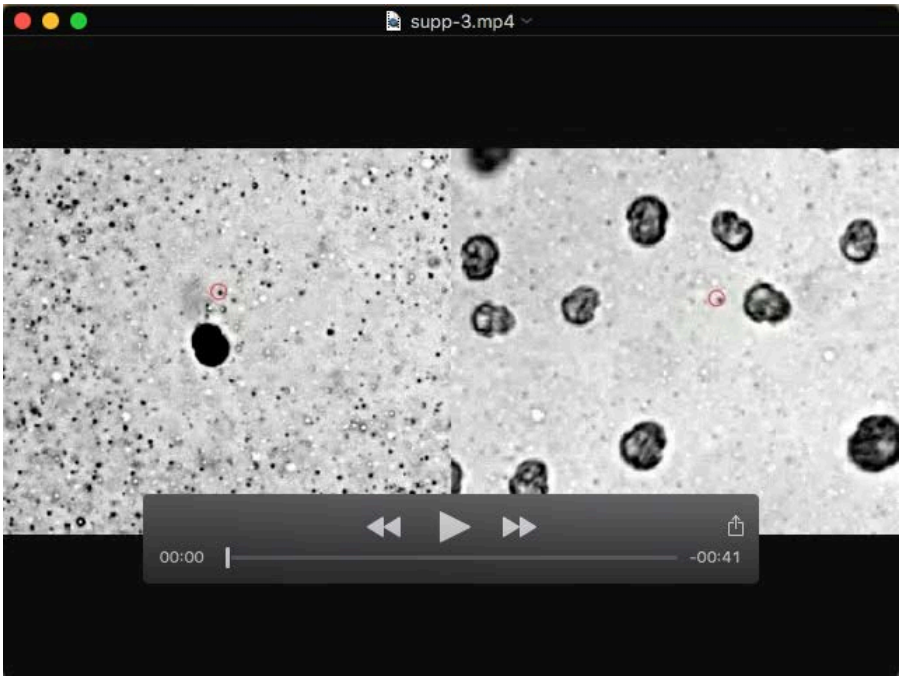

Movie 2. Tracer's trajectories influenced by the swimmers. At low algal density (left, two times slower) in contrast to the high algal density (right, normal speed).